

Vacuum energy density from a self-interacting scalar field in a Lorentz-violating Hořava-Lifshitz model

¹A. J. D. Farias Junior,^{*} ²E. R. Bezerra de Mello,[†] and ²Herondy Mota[‡]

¹*Instituto Federal de Alagoas,*

CEP: 57460-000, Piranhas, Alagoas, Brazil and

²*Departamento de Física, Universidade Federal da Paraíba,
Caixa Postal 5008, João Pessoa, Paraíba, Brazil*

In this paper we consider a massive self-interacting scalar quantum field in a Lorentz-violation scenario based on a Hořava-Lifshitz model. Specifically, we investigate the vacuum energy density and its loop correction, up to first order in the self-interaction coupling constant, and also the topological mass generation. These quantities are also analyzed in the case where the field is massless. The scalar vacuum state is perturbed by the presence of two large parallel plates, placed at a distance L from each other, due to the imposition of Dirichlet boundary condition on the two plates. To perform this study, the effective potential approach in quantum field theory is applied.

I. INTRODUCTION

One of the most important experimentally confirmed prediction in quantum field theory, is the Casimir effect. This phenomenon was first established in 1948 [1], by considering electromagnetic quantum field confined in a region between two large parallel plates. Although being electrically neutral, theoretically, these plates are attracted to each other as consequence of modification of the quantum vacuum fluctuations due to the boundary condition imposed on the field. This prediction was experimentally analyzed in [2], followed by high precisions experiments [3–9]. Casimir-like effects can emerge also by considering other kind of quantum field, such as, scalar and fermionic fields, obeying specific boundary conditions [10–12] (For an extensive review of Casimir effect see [13–15]).

Since the Theory of Relativity is the basis for quantum field theory, the standard approach for the investigation of the Casimir effect is assuming that the Lorentz symmetry is preserved. However, high energy scale theories fail to preserve the Lorentz symmetry [16, 17]. In a scenario where the Lorentz symmetry violation is allowed, the spacetime becomes anisotropic, modifying the modes of the quantum field and as a consequence, the vacuum energy density is affected. The Lorentz symmetry violation is an interesting topic which has been attracting a great deal of attention, mainly because it is an alternative to investigate new physics beyond the standard model. In Ref. [18] the authors considered a scalar field under helix boundary condition in a scenario with a CPT-even aether-type Lorentz symmetry violation to study vacuum energy density. Thermal corrections to the vacuum energy density in a Lorentz-breaking scalar field theory is considered in Ref. [19]. Considering finite temperature and an external magnetic field, the corrections to the vacuum energy due to the Lorentz violation is investigated in [20]. In Ref. [21] it was considered the Casimir like-effect with Lorentz symmetry violation in a theory with high order space derivatives. Moreover, the Lorentz symmetry violation was also considered in string theory [16] context, and in low-energy scale in Refs. [17, 22–31].

The unification of General Relativity with Quantum Mechanics remains one of the major challenges in contemporary physics. In [32], P. Horava proposed a formalism, named Horava-Lifshitz (HL) model, as an attempt to construct a renormalizable quantum field theory for gravity. In this formalism, the propagator for gravitons depends on the energy scale, introducing an anisotropy between space and time coordinates. In addition, in [33] and [34], D. Anselmi also proposed a model that violates Lorentz symmetry explicitly at high energies and is renormalizable by weighted power counting. The model contains higher space derivatives, which improve the behavior of propagators at large momenta, but no higher time derivatives. Although being different approaches, both formalism present the same feature, an explicit Lorentz violation symmetry in the higher energy scale. In this paper, even without introducing a direct coupling between the scalar field and gravity, we will refer to this formalism as being HL-like one.

The analysis of the Casimir energy associated with massless scalar quantum field confined in the region between two large and parallel plates, have been developed in [35] and [36], in the context of HL Lorentz violation. More recently, considering massive quantum field, this analysis has been developed in [37]. In this present analyzes we decided to revisit this previous investigation, i.e., the study of the vacuum energy density associated with the massive scalar

*Electronic address: antonio.farias@ifal.edu.br

†Electronic address: emello@fisica.ufpb.br

‡Electronic address: hmota@fisica.ufpb.br

quantum field. Our main objectives are to generalize results obtained in [37], considering in this model additional $\lambda\phi^4$ self-interaction of the scalar field, and not least important, to clarify some results found there. In this model we will impose that the field obeys Dirichlet boundary condition on two large and parallel plates separated by distance L . Using the path integral approach to obtain the effective potential [38], we develop the investigation of the vacuum energy density and its loop correction in the Horava-Lifshitz formalism. Furthermore, the topological mass which arises due to the boundary condition and also due to the Lorentz symmetry violation is investigated. Although the breaking of Lorentz symmetry takes place only at Planck energy scales, residual signatures of spacetime anisotropy may be observable in phenomena at lower energy scales, such as in the study of vacuum energy effects.

This paper is organized as follows: in Sec. II we review the main aspects of the Hořava-Lifshitz model, including a self-interaction potential, and the path integral formalism that we apply for the investigation we develop here, as well as the generalized zeta function technique to write the path integral in a convenient form. In Sec. III, we impose Dirichlet boundary condition on the quantum field and obtain the generalized zeta function, which allows us to write the one-loop correction and the effective potential. Sec. IV is dedicated to the analysis of the vacuum energy density for the case of both massive and massless fields, which shows a dependence on the boundary conditions obeyed by the fields and also on the Lorentz symmetry violation. In addition, the correction for the vacuum energy density is also considered in this section. Next, in Sec. IV C, we investigate the possibility of a topological mass arising due to the boundary condition, self-interaction potential and the Lorentz violation within the Hořava-Lifshitz formalism. In Sec. IV D we estimate the ratio between the parameter associated with the Lorentz violation and the length separation L between the plates. Finally in Sec. V we present our conclusions. Throughout this paper we use natural units in which both the Planck constant and the speed of light are set equal to unity, $\hbar = c = 1$.

II. HOŘAVA-LIFSHITZ THEORY AND THE ONE-LOOP CORRECTION

We first consider a massive real scalar quantum field, in a theory where the space and time have different properties by rescaling. This difference provides a spacetime anisotropy and as a consequence the Lorentz symmetry violation. The spacetime anisotropy, makes the theory invariant under the following scale transformation:

$$x \rightarrow bx, \quad t \rightarrow b^\xi t, \quad (1)$$

where ξ is a critical exponent [32]. In fact the Lorentz invariance is broken for $\xi \neq 1$; however the main objective for this violation is that for a convenient choice of ξ bigger than unity, the theory becomes free of ultraviolet divergence. Specifically focusing on the theory of gravitation, Horava, in [32] adopted $\xi = 3$. To avoid problem related with fractional derivative in this work we will assume ξ being an integer number; nonetheless, as we will see later our results are analytical function of ξ , and no restrictions need to be imposed on it.

In the 4-dimensional Euclidean spacetime and considering a self interacting field φ , we can write the action describing the system as follows [33, 34],

$$S(\varphi) = -\frac{1}{2} \int d^4x \varphi \left[-\partial_\tau^2 + (-1)^\xi l^{2(\xi-1)} (\partial_x^2 + \partial_y^2 + \partial_z^2)^\xi \right] \varphi - \int d^4x V(\varphi), \quad (2)$$

where

$$V(\varphi) = \frac{1}{2} m^2 \varphi^2 + \frac{\lambda}{4!} \varphi^4, \quad (3)$$

includes the mass and the self-interaction of the field. The parameter l in the above expression has dimension of length, and has been introduced to make the dimension of the Lagrangian density compatible. Note also that m is the mass of the field and λ is the coupling constant of the self-interaction. Our main motivation in considering the above system, is to generalize previous results developed in [37], where the authors consider massive scalar field in a HL-like model. In this present analysis we will show that the vacuum energy density vanishes for the case where ξ is an even number, besides we have also included a $\lambda\phi^4$ self-interaction term. This term introduces correction to the vacuum energy density, and is responsible for the generation of topological mass. Note that we have neglected gravity effects. In fact, our analysis presents itself as a toy model to get a grasp of how a more realistic interacting model, e.g., the electromagnetic theory with the inclusion of Lorentz violation, is supposed to be constrained.

Furthermore, in Sec. IV D, we make use of experimental data from Ref. [3] to constrain the critical exponent. The analysis of Ref. [3] does not make any reference to the nature of the quantum field, although the data better fits the electromagnetic field vacuum modes producing the Casimir effect. In spite of that, the bar error associated with the analysis makes possible to include other effects such as the contribution of other quantum fields, finite temperature effects, plates roughness, and so on. This would help to improve the obtained constraints in Ref. [3].

In order to analyze the vacuum energy and the generation of topological mass associated with the system under consideration, we will construct the effective potential by expanding the action about the background field, Φ , by setting $\varphi = \Phi + \phi$, with ϕ representing the quantum fluctuations. This provides a series expansion as shown below,

$$V_{\text{eff}}(\Phi) = \sum_n V^{(n)}(\Phi). \quad (4)$$

In our analysis we are interested up to the second order in the expansion. Note that, in this paper, we are adopting natural units.

As it is well known the zero order term in (4) corresponds to the tree level contribution, and the first and second ones to the 1- and 2-loop corrections, respectively. For a more detailed explanation about this formalism, see [38–43]. The first order contribution, $V^{(1)}(\Phi)$, can be written in terms of path integral as:

$$V^{(1)}(\Phi) = -\frac{1}{\Omega_4} \ln \int \mathcal{D}\varphi \exp \left[-\frac{1}{2} \int d^4x \varphi(x) \hat{A} \varphi(x) \right], \quad (5)$$

where Ω_4 is the 4-dimensional volume of the Euclidean spacetime, which depends on the conditions imposed on the fields. In our case the operator \hat{A} is given by,

$$\hat{A} = -\partial_\tau^2 + (-1)^\xi l^{2(\xi-1)} (\partial_x^2 + \partial_y^2 + \partial_z^2)^\xi + V''(\Phi). \quad (6)$$

The double prime notation in $V''(\Phi)$, stands for the second derivative of $V(\varphi)$ with respect to the field φ calculated at Φ , which is the fixed background field. Then, for the theory we consider, $V''(\Phi)$ takes the following form

$$V''(\Phi) = m^2 + \frac{\lambda}{2} \Phi^2. \quad (7)$$

Regarding the one loop correction to the effective potential we will use the zeta-function technique to perform the calculations. Thus, denoting by Λ_σ the set of the eigenvalues of the operator \hat{A} , the corresponding zeta function reads:

$$\zeta(s) = \sum_\sigma \Lambda_\sigma^{-s}, \quad (8)$$

In the above expression σ represents the complete set of quantum numbers that characterize the eigenfunction of \hat{A} . The summation symbol denotes sum over discrete quantum numbers, and integration over continuous ones. Once we construct the generalized zeta function in Eq. (8), we write the one-loop correction to the effective potential in the following form [40, 43, 44]:

$$V^{(1)}(\Phi) = -\frac{1}{2\Omega_4} [\zeta'(0) + \zeta(0) \ln \nu^2]. \quad (9)$$

The notations $\zeta(0)$ and $\zeta'(0)$ stand for the generalized zeta function and its derivative with respect to s , evaluated at $s = 0$, respectively. The parameter ν has dimension of mass which is to be removed by a renormalization procedure.

At this point we would like to mention that, although we have used an Euclidean extension of the Klein-Gordon operator, Eq. (6), the effective potential obtained is a real function. Thus, the mathematical approach adopted here, does not affect the physical result.

On the other hand, in order to calculate the two-loop correction to the effective potential we will use Feynman graphs. As we are interested only in the vacuum contribution, this correction can be written in the terms of the generalized zeta function [41–43]. We postpone the explicit form of $V^{(2)}(\Phi)$ until Section IV B.

III. DIRICHLET BOUNDARY CONDITION, GENERALIZED ZETA FUNCTION AND THE ONE-LOOP CORRECTION

In this section, we apply the Dirichlet boundary condition on two parallel large plates, separated by a distance L along the z direction. Within this configuration, the scalar field φ satisfies the following restriction:

$$\varphi(\tau, x, y, 0) = \varphi(\tau, x, y, L) = 0. \quad (10)$$

The above condition implies that the eigenvalues of the operator \hat{A} given in Eq. (6) takes the form,

$$\Lambda_\sigma = k_\tau^2 + (-1)^{2\xi} l^{2(\xi-1)} \left[k_x^2 + k_y^2 + \left(\frac{\pi n}{L} \right)^2 \right]^\xi + V''(\Phi). \quad (11)$$

Note that the momentum in z has been discretized and n assumes non-negative integers values, that is, $n = 1, 2, 3, \dots$. The set of quantum modes in this case is given by $\sigma = (k_\tau, k_x, k_y, n)$, with (k_τ, k_x, k_y) being the continuous momenta.

The eigenvalues given in Eq. (11) are used to construct the generalized zeta function (8), which is written as,

$$\zeta(s) = \frac{\Omega_3}{(2\pi)^3} \sum_{n=1}^{\infty} \int dk_\tau dk_x dk_y \left\{ k_\tau^2 + (-1)^{2\xi} l^{2(\xi-1)} \left[k_x^2 + k_y^2 + \left(\frac{\pi n}{L} \right)^2 \right]^\xi + V''(\Phi) \right\}^{-s}. \quad (12)$$

The quantity Ω_3 represents the 3-dimensional volume associated with the Euclidean time coordinate τ and the spatial coordinates x and y . In order to obtain the generalized zeta function in a more convenient form, we start by using the following identity:

$$w^{-s} = \frac{2}{\Gamma(s)} \int_0^\infty dt t^{2s-1} e^{-wt^2}, \quad (13)$$

where $\Gamma(s)$ is the gamma function. This allows us to perform the Gaussian-like integral in the k_τ variable present in Eq. (12), providing that,

$$\zeta(s) = \frac{2\Omega_3\pi^{\frac{1}{2}}}{(2\pi)^3 \Gamma(s)} \sum_{n=1}^{\infty} \int dk_x dk_y \int_0^\infty dt t^{2s-2} \exp \left\{ -bt^2 \left[\left(k_x^2 + k_y^2 + \left(\frac{\pi n}{L} \right)^2 \right)^\xi + \frac{V''(\Phi)}{b} \right] \right\}, \quad (14)$$

where we have defined the quantity b as,

$$b = l^{2(\xi-1)}. \quad (15)$$

At this stage, it is more appropriate to write the k_x and k_y integrals in polar coordinates and perform the integral in the polar angle. After we perform two changes of integration variables, namely, $\chi = \frac{b\pi^{2\xi}}{L^{2\xi}} t^2$ and $\omega = \chi \left[\left(\frac{kL}{\pi} \right)^2 + n^2 \right]^\xi$, we end up with the following expression for the generalized zeta function:

$$\zeta(s) = \frac{\Omega_3 b^{\frac{1}{2}-s} \pi^{\frac{1}{2}-2\xi s+\xi}}{8\xi L^{2-2\xi s+\xi} \Gamma(s)} \sum_{n=1}^{\infty} \int_0^\infty d\chi \chi^{s-\frac{3}{2}-\frac{1}{\xi}} e^{-\chi U} \int_{\chi n^{2\xi}}^\infty d\omega \omega^{\frac{1}{\xi}-1} e^{-\omega}, \quad (16)$$

where we set U in the form,

$$U = \frac{L^{2\xi}}{b\pi^{2\xi}} V''(\Phi). \quad (17)$$

In the generalized zeta function given in Eq. (16), we identify the incomplete gamma function $\Gamma(\alpha, x)$ defined as [45],

$$\Gamma(\alpha, x) = \int_x^\infty dt t^{\alpha-1} e^{-t} = e^{-x} \Psi(1-\alpha, 1-\alpha, x), \quad \text{Re } \alpha > 0, \quad (18)$$

where the function $\Psi(\alpha, \beta, z)$ is a combination of confluent hypergeometric functions ${}_1F_1(\alpha, \gamma, z)$ [45], that is,

$$\Psi(\alpha, \beta, z) = \frac{\Gamma(1-\gamma)}{\Gamma(\alpha-\gamma+1)} {}_1F_1(\alpha, \gamma, z) + \frac{\Gamma(1-\gamma)}{\Gamma(\alpha)} z^{1-\gamma} {}_1F_1(\alpha-\gamma+1, 2-\gamma, z). \quad (19)$$

Hence, we obtain the following expression for the generalized zeta function:

$$\zeta(s) = \frac{\Omega_3 b^{\frac{1}{2}-s} \pi^{\frac{1}{2}-2\xi s+\xi}}{8\xi \Gamma(s) L^{2-2\xi s+\xi}} \sum_{n=1}^{\infty} \int_0^\infty d\tau \frac{\tau^{s-\frac{3}{2}-\frac{1}{\xi}}}{n^{2\xi s-\xi-2}} e^{-\tau(1+\frac{U}{n^{2\xi}})} \Psi\left(1-\frac{1}{\xi}, 1-\frac{1}{\xi}, \tau\right), \quad (20)$$

where we have made another change of variable, namely, $\tau = tn^{2\xi}$. The form of the generalized zeta function above suggests the use of the integral below [45], i.e.,

$$\int_0^\infty t^{b-1} e^{-zt} \Psi(a, c, t) dt = \frac{\Gamma(b) \Gamma(b-c+1) z^{-b}}{\Gamma(a+b-c+1)} {}_2F_1(a, b, a+b-c+1, 1-z^{-1}). \quad (21)$$

Therefore, with the help of Eq. (21), we can rewrite the generalized zeta function, Eq. (20), as

$$\begin{aligned} \zeta(s) &= \frac{\Omega_3 \pi^{\frac{1}{2}-2\xi s + \xi} b^{\frac{1}{2}-s} \Gamma\left(s - \frac{1}{2} - \frac{1}{\xi}\right) \Gamma\left(s - \frac{1}{2}\right)}{8\xi L^{2-2\xi s + \xi} \Gamma(s) \Gamma\left(s + \frac{1}{2} - \frac{1}{\xi}\right)} \\ &\times \sum_{n=1}^{\infty} (n^{2\xi} + U)^{\frac{1}{2} + \frac{1}{\xi} - s} {}_2F_1\left(1 - \frac{1}{\xi}, s - \frac{1}{2} - \frac{1}{\xi}, s + \frac{1}{2} - \frac{1}{\xi}, \frac{U}{n^{2\xi} + U}\right), \end{aligned} \quad (22)$$

where the function ${}_2F_1(\alpha, \beta, \gamma, z)$ is the hypergeometric function [45]. The sum above is clearly divergent so that we need a renormalization method to subtract the infinite contribution and only work with the finite part of the generalized zeta function.

In order to perform the sum over the quantum number n in Eq. (22) and obtain a finite contribution, we use the Abel-Plana summation formula [13, 36, 46, 47]. The calculations using this formula are described in Appendix A where it is shown that there are three resulting terms, but only one provides a finite vacuum energy density, which is given by

$$\begin{aligned} \zeta_0(s) &= - \frac{\Omega_3 \pi^{\frac{1}{2} + \xi - 2\xi s} b^{\frac{1}{2} - s} \Gamma\left(s - \frac{1}{2} - \frac{1}{\xi}\right) \Gamma\left(s - \frac{1}{2}\right) \sin\left[\pi\left(\frac{\xi}{2} + 1 - \xi s\right)\right]}{4\xi L^{2+\xi-2\xi s} \Gamma(s) \Gamma\left(s + \frac{1}{2} - \frac{1}{\xi}\right)} \\ &\times \int_{U^{\frac{1}{2\xi}}}^{\infty} dx \mathcal{F}_s(\xi, U, x), \end{aligned} \quad (23)$$

where we have defined the function $\mathcal{F}_s(\xi, U, x)$ as

$$\mathcal{F}_s(\xi, U, x) = \frac{(x^{2\xi} - U)^{\frac{1}{2} + \frac{1}{\xi} - s}}{e^{2\pi x} - 1} {}_2F_1\left(1 - \frac{1}{\xi}, s - \frac{1}{2} - \frac{1}{\xi}, s + \frac{1}{2} - \frac{1}{\xi}, \frac{U}{U - x^{2\xi}}\right). \quad (24)$$

With the finite generalized zeta function obtained above, we proceed to calculate the one-loop correction to the effective potential from Eq. (9). In order to do so, we have to evaluate the generalized zeta function above and its derivative at $s = 0$, that is, $\zeta(0)$ and $\zeta'(0)$. From the calculations presented in Appendix A, we find that,

$$\begin{aligned} \zeta_0(0) &= 0, \\ \zeta'_0(0) &= \frac{\Omega_3 \pi^{1+\xi} b^{\frac{1}{2}} \sin(\pi\xi/2)}{(\xi + 2) L^{2+\xi}} \int_{U^{\frac{1}{2\xi}}}^{\infty} dx \mathcal{F}_0(\xi, U, x), \end{aligned} \quad (25)$$

where we should remember that the quantity U is given in Eq. (17) together with (7). We should also emphasize that the contribution presented in Eq. (25) is the one that gives rise to the vacuum energy density, as we shall see.

Due to the renormalization procedure performed using Abel-Plana summation formula [36], the one-loop correction to the effective potential takes into consideration only the contribution given in Eq. (25), therefore the one-loop correction, Eq. (9), is written in the following manner:

$$V^{(1)}(\Phi) = - \frac{\pi^{1+\xi} l^{\xi-1} \sin(\pi\xi/2)}{2(\xi + 2) L^{3+\xi}} \int_{U^{\frac{1}{2\xi}}}^{\infty} dx \mathcal{F}_0(\xi, U, x). \quad (26)$$

Hence, the renormalized effective potential for a massive self-interacting scalar field within the Hořava-Lifshitz formalism takes the form

$$V_{\text{eff}}^{\text{R}}(\Phi) = \frac{1}{2} m \Phi^2 + \frac{\lambda}{4!} \Phi^4 - \frac{\pi^{1+\xi} l^{\xi-1} \sin(\pi\xi/2)}{2(\xi + 2) L^{3+\xi}} \int_{U^{\frac{1}{2\xi}}}^{\infty} dx \mathcal{F}_0(\xi, U, x). \quad (27)$$

An interesting aspect to be noted in our result is that it has not been necessary to introduce counterterms in the action (2) to obtain the renormalized effective potential above, in contrast with Ref. [41] in the case $\xi = 1$. In the latter, besides $\zeta_0(0) \neq 0$, $\zeta'_0(0)$ contains logarithmic divergence when $\Phi = 0$ and also a dependence on the scale ν present here in Eq. (9). This kind of terms need to be removed which, in the context of the effective potential approach, is usually done by introducing counterterms in the action. The absence of this logarithmic divergence in our case is a characteristic of the H-L model adopted. Thus, the counterterms are needless. Although we have considered ξ being an integer number, our result above is an analytical function of it; consequently by an analytical continuation Eq. (27) remains valid for any value of ξ .

Once we obtain the explicit form of the renormalized effective potential, up to one-loop correction, we can calculate the vacuum energy density and also analyze a possible generation of topological mass. Let us do this in the proceeding sections.

IV. VACUUM ENERGY DENSITY AND TOPOLOGICAL MASS

In this section we investigate the vacuum energy density for a real scalar field, its corresponding order λ correction, which is in fact the contribution from the two-loop correction to the effective potential calculated at the vacuum state, and also the topological mass. Next, we consider first the vacuum energy density.

A. Vacuum energy density for the massive field

Upon using the renormalized effective potential (27) obtained in the previous section, we can calculate the vacuum energy density directly by taking the vacuum state, i.e., $\Phi = 0$. Hence, we obtain the vacuum energy density in the following form:

$$\begin{aligned}\mathcal{E}_0 &= V_{\text{eff}}^R(0) \\ &= -\frac{\pi \sin(\pi\xi/2)}{2L^4(\xi+2)R_\xi} \int_{U_0^{\frac{1}{2\xi}}}^{\infty} dx \mathcal{F}_0(\xi, U_0, x),\end{aligned}\quad (28)$$

where the function $\mathcal{F}_0(\xi, U_0, x)$ is presented in Eq. (24), with U_0 given by,

$$\begin{aligned}U_0 = U|_{\Phi=0} &= (mL)^2 \left[\frac{1}{\pi^\xi} \left(\frac{L}{l} \right)^{\xi-1} \right]^2 \\ &= (mL)^2 R_\xi^2.\end{aligned}\quad (29)$$

As we can see, the vacuum energy density given in Eq. (28) can be positive or negative depending on the value of the parameter ξ which, as seen in Appendix A, assumes only odd values. The expression (28) is the general result for the vacuum energy density, for a massive scalar field within the Hořava-Lifshitz formalism, satisfying Dirichlet boundary conditions on the parallel plates. Unfortunately, it is not possible to solve the integral in Eq. (28) for all odd values of ξ , except the standard case $\xi = 1$ that preserves the Lorentz symmetry.

Let us now closely consider the standard case in which the critical exponent is set equal to the unity, i.e., $\xi = 1$. Since $F(0, \beta, \gamma, x) = 1$, the vacuum energy density in Eq. (28) becomes

$$\mathcal{E}_0(\xi = 1) = -\frac{m^4}{6\pi^2} \sum_{n=1}^{\infty} \int_1^{\infty} dy (y^2 - 1)^{\frac{3}{2}} e^{-2nmLy},\quad (30)$$

where we have performed the change of integration variable, $y = xU_0^{-\frac{1}{2}}$. Note also that the sum in n of the exponential above provides the expression $(e^{2mLy} - 1)^{-1}$.

The integral in Eq. (30) can be performed with the help of the following identity [45]:

$$\int_1^{\infty} dx (x^2 - 1)^{\nu-1} e^{-\mu x} = \pi^{-\frac{1}{2}} \left(\frac{2}{\mu} \right)^{\nu-\frac{1}{2}} \Gamma(\nu) K_{\nu-\frac{1}{2}}(\mu),\quad (31)$$

where $K_2(\mu)$ is the Macdonald function or the modified Bessel function of the second kind [48]. Hence, the vacuum energy density for the case $\xi = 1$ takes the form,

$$\mathcal{E}_0(\xi = 1) = -\frac{m^2}{8\pi^2 L^2} \sum_{n=1}^{\infty} n^{-2} K_2(2nmL).\quad (32)$$

The above result is in agreement with the standard result where the Lorentz symmetry is preserved which we can check, for instance, in Refs. [14, 49, 50].

In order to construct a graph for the vacuum energy density given in Eq. (28) as a function of mL , it is more convenient to express it in terms of the variable, $z = x^{2\xi} - U$. Hence, Eq. (28) can be written as

$$\mathcal{E}_0 = -\frac{\pi \sin(\pi\xi/2)}{4L^4\xi(\xi+2)R_\xi} \int_0^{\infty} dz \frac{z^{\frac{1}{2}+\frac{1}{\xi}} (z+U_0)^{\frac{1}{2\xi}-1}}{\left[e^{2\pi(z+U_0)^{\frac{1}{2\xi}}} - 1 \right]} {}_2F_1 \left(1 - \frac{1}{\xi}, -\frac{1}{2} - \frac{1}{\xi}, \frac{1}{2} - \frac{1}{\xi}, -\frac{U_0}{z} \right),\quad (33)$$

where U_0 has been defined in terms of R_ξ in Eq. (29). Thus, we shall now consider graphs of the dimensionless vacuum energy density, $E(mL) = \frac{4L^4}{\pi} \mathcal{E}_0$, as a function of mL .

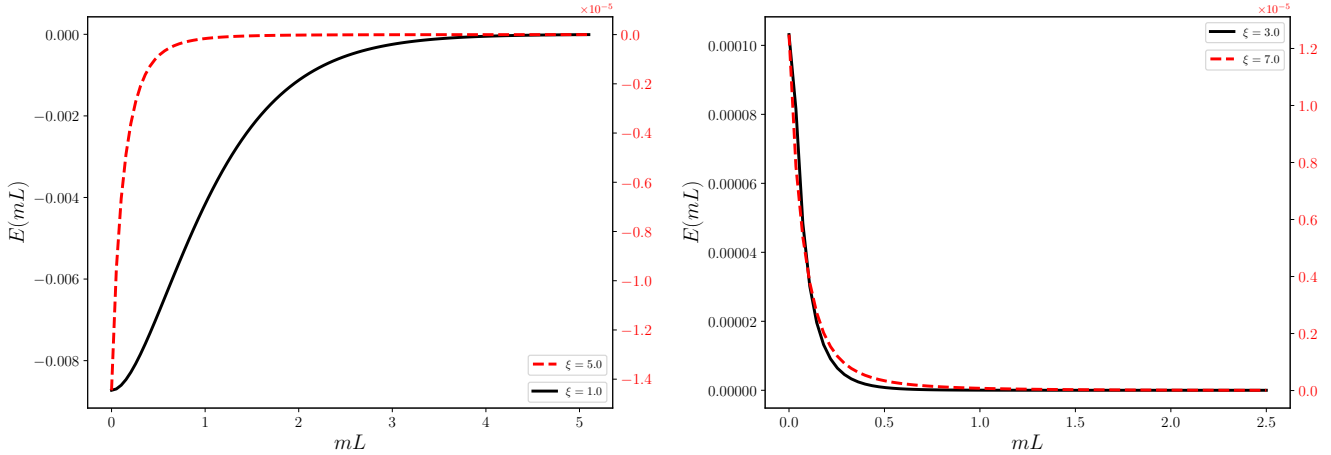


FIG. 1: Graphs of the dimensionless vacuum energy density $E(mL) = \frac{4}{\pi}L^4\mathcal{E}_0$, as a function of mL . The graph on the left considers the values $\xi = 1.0$ (solid black curve) and $\xi = 5.0$ (dashed red curve), while the plot on the right considers the values $\xi = 3.0$ (solid black curve) and $\xi = 7.0$ (dashed red curve). The scale of each curve is shown in the vertical axes with the correspondent color.

In Fig.1 we exhibit graphs of the dimensionless vacuum energy density $E(mL)$, as a function of mL , considering the values $\xi = 1, 3, 5, 7$. The graph on the left shows the curves for $\xi = 1$ and $\xi = 5$. The solid black curve stands for the case $\xi = 1$ while the dashed red curve for the case $\xi = 5$. Similarly, the graph on the right considers the cases where $\xi = 3$ (solid black line) and $\xi = 7$ (dashed red line). These plots also show a strong decay of the vacuum energy density with mL . Explicitly in (32) we can see an exponential decay for $mL \gg 1$. Note that the scale of each curve is correspondently shown on the left and on the right of the vertical axes. Although in section IV D we make an estimation on the ratio $\frac{1}{L}$ by using experimental data, for simplicity, we have taken values of R_ξ such that

$$R_1 = 1/\pi, \quad R_3 = 24, \quad R_5 = 32, \quad R_7 = 80, \quad R_9 = 260. \quad (34)$$

Therefore, the plot on the left of Fig.1 shows that the order of the vacuum energy density, in absolute values, greatly decreases compared with the standard case $\xi = 1$. This aspect is also shown in the plot on the right, which also reveals that for values $\xi = 3, 7$ the vacuum energy density gives rise to a repulsive force, in contrast with the cases $\xi = 1, 5$.

Let us now consider the massless scalar field case. For this, we should take the limit $m \rightarrow 0$ ($U_0 \rightarrow 0$) in Eq. (28). This provides

$$\mathcal{E}_0 = -\frac{\pi^{1+\xi}l^{(\xi-1)}\sin(\pi\xi/2)}{2(\xi+2)L^{3+\xi}}\int_0^\infty\frac{x^{\xi+2}}{e^{2\pi x}-1}dx. \quad (35)$$

The integral above can be performed by using the following relation [45]:

$$\int_0^\infty dx \frac{x^{\nu-1}}{e^{\mu x}-1} = \mu^{-\nu}\Gamma(\nu)\zeta_R(\nu), \quad \mu > 0, \quad \nu > 1, \quad (36)$$

where $\zeta_R(s)$ is the Riemann zeta function. Therefore, we obtain the vacuum energy density for the massless field as

$$\mathcal{E}_0 = -\frac{l^{(\xi-1)}\sin(\pi\xi/2)}{2\xi+4\pi^2L^{3+\xi}}\Gamma(\xi+2)\zeta_R(\xi+3), \quad (37)$$

which is in agreement with the result found in Ref. [36].

We want now go further to consider the correction to the vacuum energy density, which is proportional to the self-interaction coupling constant λ , in linear order. This contribution comes from the two-loop correction to the effective potential, as we shall see below.

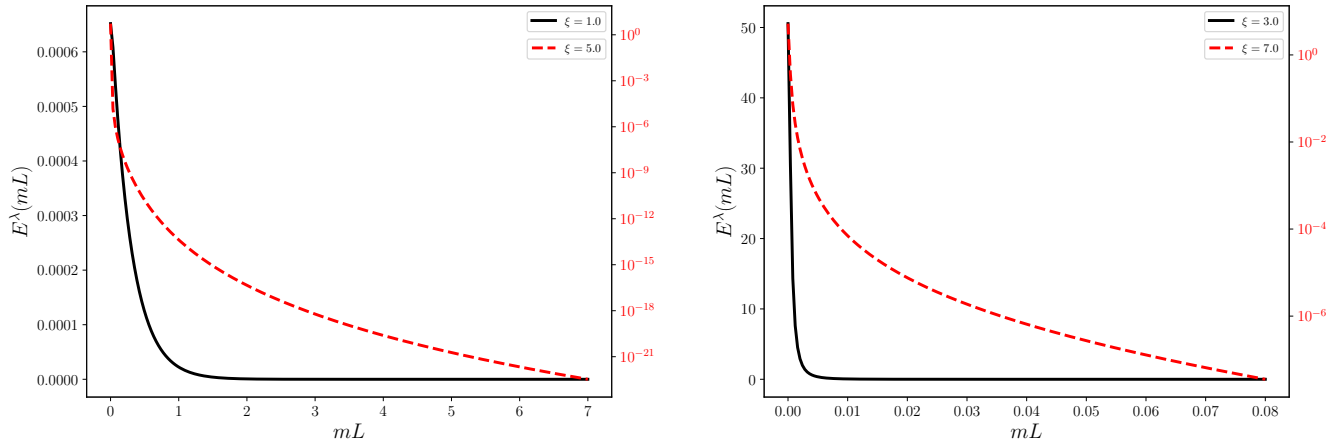


FIG. 2: Graphs of the dimensionless order- λ contribution to the vacuum energy density $E^\lambda(mL) = \frac{128}{\lambda\pi^2} L^4 \mathcal{E}_0^\lambda$, as a function of mL . The graph on the left considers the values $\xi = 1.0$ (solid black curve) and $\xi = 5.0$ (dashed red curve), while the plot on the right considers the values $\xi = 3.0$ (solid black curve) and $\xi = 7.0$ (dashed red curve). The scale of each curve is shown in the vertical axes with the correspondent color.

B. Order- λ correction to the vacuum energy density

The two-loop correction to the effective potential at the vacuum state $\Phi = 0$, provides a order- λ loop correction to the vacuum energy density, Eq. (28). This contribution can be written in terms of the finite generalized zeta function (23) as [18, 42, 43],

$$\mathcal{E}_0^\lambda = V^{(2)}(0) = \frac{\lambda}{8} \left[\frac{\zeta_0(1)}{\Omega_4} \right]_{\Phi=0}^2, \quad (38)$$

where

$$\frac{\zeta_0(1)}{\Omega_4} \Big|_{\Phi=0} = -\frac{\pi^{1-\xi} \sin(\pi\xi/2)}{2(\xi-2)l^{(\xi-1)}L^{3-\xi}} \int_{U_0^{\frac{1}{2\xi}}}^{\infty} dx \mathcal{F}_1(\xi, U_0, x), \quad (39)$$

with $\Omega_4 = \Omega_3 L$. This leads to the following order- λ correction to the vacuum energy density:

$$\mathcal{E}_0^\lambda = \frac{\lambda\pi^2 R_\xi^2}{32L^4(\xi-2)^2} \left[\int_{U_0^{\frac{1}{2\xi}}}^{\infty} dx \mathcal{F}_1(\xi, U_0, x) \right]^2, \quad (40)$$

where R_ξ has been defined in Eq. (29) and the function $\mathcal{F}_s(\xi, U_0, x)$ in Eq. (24). In order to construct a graph for the above correction it is useful to use the same change of variable as in Eq. (33).

In Fig.2 we have plotted the dimensionless order- λ correction to the vacuum energy density $E^\lambda(mL) = \frac{128}{\lambda\pi^2} L^4 \mathcal{E}_0^\lambda$ as a function of mL . The graph on the left considers the case $\xi = 1$ represented by the solid black curve, while the case $\xi = 5$ is represented by the dashed red curve. Similarly, the graph on the right shows the cases $\xi = 3$ (solid black curve) and $\xi = 7$ (dashed red curve). For both plots the scale of the vacuum energy density is shown in the vertical axes with the correspondent color. Note that in both plots the red vertical axis is in logarithmic scale. Note also that the values given in Eq. (34) are also considered here. We can again see that the scale of the vacuum energy density greatly decreases in each case, as compared with the standard case $\xi = 1$. The graphs above also show that the correction to the vacuum energy density goes to zero as $mL \rightarrow \infty$. However, exactly at $mL = 0$ (massless case), the correction diverges for $\xi > 1$, as we shall see more clearly below.

We turn now to the massless scalar field case, which can be obtained by taking the limit $m \rightarrow 0$ ($U_0 \rightarrow 0$) of Eq. (40). This gives

$$\mathcal{E}_0^\lambda = \frac{\lambda\pi^{2-2\xi}}{32(\xi-2)^2 l^{2(\xi-1)} L^{6-2\xi}} \left[\int_0^\infty dx \frac{x^{2-\xi}}{e^{2\pi x} - 1} \right]^2. \quad (41)$$

Note that the integral above does not converge for $\xi > 1$. This is a consequence of the Hořava-Lifshitz model adopted here, which helps to eliminate ultraviolet divergences but as a consequence brings infrared ones in the massless limit of Eq. (40). The question whether this infrared divergence can be treated will be considered elsewhere.

Fortunately, the integral in Eq. (41) converges for $\xi = 1$ and provides the standard result where the Lorentz symmetry is preserved [41]. So, let us first consider $\xi = 1$ in Eq. (40). In this case, we obtain the following result:

$$\begin{aligned} \mathcal{E}_0^\lambda (\xi = 1) &= \frac{\lambda m^4}{32\pi^4} \left[\sum_{n=1}^{\infty} \int_1^{\infty} dy (y^2 - 1)^{\frac{1}{2}} e^{-2nmLy} \right]^2 \\ &= \frac{\lambda m^2}{128\pi^4 L^2} \left[\sum_{n=1}^{\infty} n^{-1} K_1(2nmL) \right]^2, \end{aligned} \quad (42)$$

which is in agreement with the results found in Ref. [41] in the case with no Lorentz violation. Note that we have used again the change of variable $y = xU_0^{-\frac{1}{2}}$, and also Eq. (31). This is similar to what we have done in Eq. (30).

In addition, from Eq. (41), for a massless scalar field, we have

$$\mathcal{E}_0^\lambda (\xi = 1) = \frac{\lambda}{18432L^4}, \quad (43)$$

which is also in agreement with Ref. [41].

In general the zeta-function, $\zeta_0(s)$, evaluated at $s = 1$ presents a divergent contribution, as it was pointed out in [41]. This contribution needs to be subtracted by some regularization procedure. However, in the H-L context, there is no such divergence, and all results are finite, as we have shown above.

In the next section we consider an analysis for the topological mass generated by the boundary condition. We, thus, expect the result will depend on the self-interaction coupling λ and the Lorentz violation parameter l .

C. Topological mass for the massive field

In this section we investigate the topological mass which arises due to the boundary condition, self-interaction potential and the Lorentz violation within the Hořava-Lifshitz formalism used here.

The topological mass squared of the field can be written as the second derivative of the effective potential, evaluate at the vacuum state, that is, $\Phi = 0$ [40]. Hence, using the effective potential given in Eq. (27) we write the topological mass as,

$$m_{\text{T}}^2 = \left. \frac{d^2 V_{\text{eff}}^{\text{R}}(\Phi)}{d\Phi^2} \right|_{\Phi=0}. \quad (44)$$

In order to perform the derivative of the effective potential, we have to apply the Leibniz rule [51]. The final result reads,

$$m_{\text{T}}^2 = m^2 - \frac{\lambda\pi \sin(\pi\xi/2)}{4\xi L^4 m^2 R_\xi} \int_{U_0^{-\frac{1}{2\xi}}}^{\infty} dx \left[\mathcal{F}_0(\xi, U_0, x) - \frac{x^2 (x^{2\xi} - U_0)^{\frac{1}{2}}}{e^{2\pi x} - 1} \right]. \quad (45)$$

The expression above, as expected, goes to zero as $mL \rightarrow \infty$ for any odd value of ξ . However, at $mL = 0$, that is, in the massless case, it diverges for $\xi > 1$ as a consequence of infrared divergences that appear due to the Hořava-Lifshitz model adopted here. This problem, on the other hand, does not exist if we take $\xi = 1$, which is the standard case where the Lorentz symmetry is preserved. Hence, for $\xi = 1$, Eq. (45) can be written as

$$m_{\text{T}}^2 = m^2 + \frac{\lambda m^2}{4\pi^2} \sum_{n=1}^{\infty} \int_1^{\infty} dy (y^2 - 1)^{\frac{1}{2}} e^{-2nmLy}, \quad (46)$$

where we have expressed $(e^{2\pi x} - 1)^{-1}$ as a sum in n of the exponential above. We have also performed the change of variable $y = xU_0^{-\frac{1}{2}}$, similar to Eq. (30). Now, by using Eq. (31) we find

$$m_{\text{T}}^2 (\xi = 1) = m^2 \left[1 + \frac{\lambda}{8\pi^2 mL} \sum_{n=1}^{\infty} n^{-1} K_1(2nmL) \right], \quad (47)$$

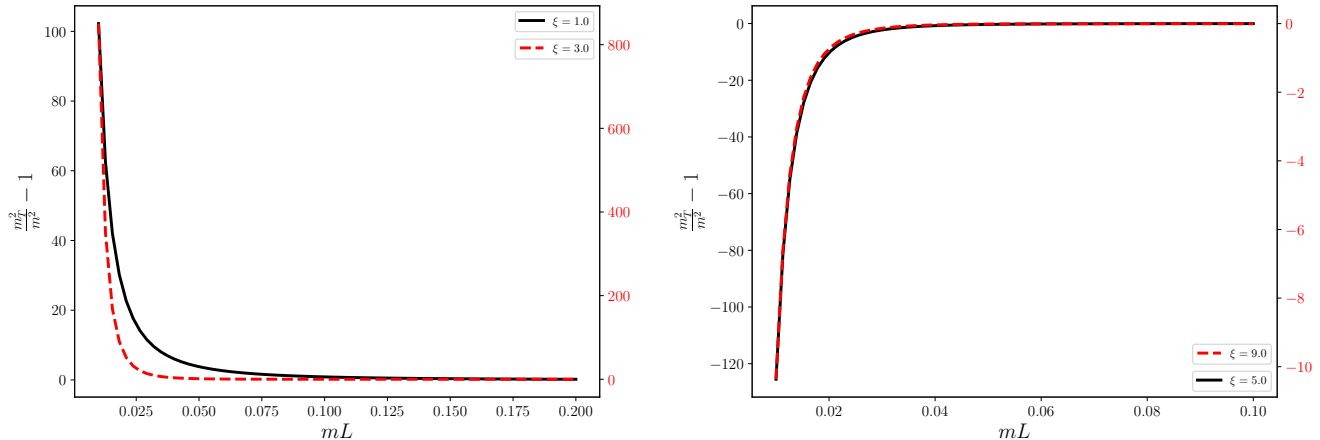


FIG. 3: Graphs of the dimensionless topological mass $\frac{m_T^2}{m^2} - 1$, as a function of mL . The graph on the left considers the values $\xi = 1.0$ (solid black curve) and $\xi = 3.0$ (dashed red curve), while the plot on the right considers the values $\xi = 5.0$ (solid black curve) and $\xi = 9.0$ (dashed red curve). The scale of each curve is shown in the vertical axes with the correspondent color.

which is in agreement with known results found in the literature [41]. Note that the massless scalar field case for the topological mass follows directly from Eq. (47).

Nevertheless, in order to better notice the infrared divergences that appear in the massless limit of Eq. (45), let us take the limit $mL \rightarrow 0$ ($U_0 \rightarrow 0$) of Eq. (45). For this, we should consider the following expansion for small mL :

$$\left[(e^{2\pi x} - 1) \mathcal{F}_0(\xi, U_0, x) - x^2 (x^{2\xi} - U_0)^{\frac{1}{2}} \right] \simeq \frac{\xi x^{2-\xi}}{(\xi - 2)} U_0 + O(U_0^2). \quad (48)$$

Consequently, Eq. (45) becomes

$$m_T^2 = -\frac{\lambda \pi \sin(\pi\xi/2) R_\xi}{4(\xi - 2) L^2} \int_0^\infty \frac{dx x^{2-\xi}}{(e^{2\pi x} - 1)}. \quad (49)$$

As we can see, the integral above does not converge for $\xi > 1$. However, for $\xi = 1$, we have

$$m_T^2(\xi = 1) = \frac{\lambda}{96L^2}, \quad (50)$$

which is a known result [41]. It is clear now that, for any odd values of ξ , the expression in Eq. (45) is only valid for $m > 0$. On the other hand, for $\xi = 1$, it provides known results for both the massive and massless scalar field cases.

The generation of topological mass, will reinforce the already strong decay in the vacuum energy density, as mentioned before. In this sense the search of this effect becomes experimentally much harder.

In order to plot the expression in Eq. (45) with respect to mL it is again useful to use the same change of variable as in Eq. (33). The correspondent plots are exhibited in Fig.3. Note that we have plotted only the second term on the r.h.s. of Eq. (45). The graphs clearly show that the topological mass goes to zero as $mL \rightarrow \infty$, as it should be. However, for $mL \rightarrow 0$, the topological mass goes to infinity indicating the presence of infrared divergences in the massless limit. Moreover, as we can see, for some values of ξ like $\xi = 5, 9$, the values of the topological mass become negative which may indicate that an analysis of vacuum stability is necessary within a model where the scalar field considered here interacts with a second field, similar what has been done in Refs. [43, 52].

D. Estimative for the ratio $(l/L)^{\xi-1}$

In this section we consider the experimental results presented in [3] in order to estimate the ratio $(l/L)^{\xi-1}$. Hence, from Ref. [3], we consider

$$\Delta\nu^2 = -\frac{C_{\text{Cas}}}{L^5}, \quad (51)$$

ξ	$\xi = 3$	$\xi = 5$	$\xi = 7$	$\xi = 9$
$(\frac{l}{L})^{\xi-1}$	$(\frac{l}{L})^2 = 1.32588 \times 10^{-27}$	$(\frac{l}{L})^4 = 9.59569 \times 10^{-29}$	$(\frac{l}{L})^6 = 4.27789 \times 10^{-30}$	$(\frac{l}{L})^8 = 1.2973 \times 10^{-31}$

TABLE I: $(l/L)^{\xi-1}$ as a function of ξ .

where $C_{\text{Cas}} = (2.34 \pm 0.34) \times 10^{-28} \text{ Hz}^2\text{m}^5$. The connection between the vacuum energy density given in Eq. (37), with the Casimir energy E_0 is given by [41],

$$E_0 = AL\mathcal{E}_0, \quad (52)$$

where A is the area of the plates. The Casimir force, F_0 , is obtained via derivative of the Casimir energy with respect to the distance L , and the Casimir pressure, P_0 , is the Casimir force divided by the area A , i.e.,

$$P_0 = \frac{F_0}{A} = -\frac{1}{A} \frac{\partial E_0}{\partial L}. \quad (53)$$

According to the method proposed in Ref. [53], we can write the relation between $\Delta\nu^2$ and E_0 as,

$$\Delta\nu^2 = -\frac{A}{4\pi^2 m_{\text{eff}}} \frac{\partial P_0}{\partial L} = \frac{A}{4\pi^2 m_{\text{eff}}} \frac{\partial}{\partial L} \left(\frac{1}{A} \frac{\partial E_0}{\partial L} \right), \quad (54)$$

where m_{eff} is an effective mass and the ratio A/m_{eff} is experimentally estimated in [3], that is,

$$\frac{A}{m_{\text{eff}}} \approx 1.746 \text{ Hz}^2\text{m}^3\text{N}^{-1}. \quad (55)$$

Note that the expression in Eq. (54) is the general definition of $\Delta\nu^2$ appearing in Eq. (51). This is discussed, for instance, in Ref. [53] and will be applied to our case.

Using the result obtained in Eq. (37) for the vacuum energy density in the case of massless scalar field, together with the relation expressed by Eq. (52), we find the vacuum pressure for a massless field in the Hořava-Lifshitz model considered here as

$$P_0 = -\sin\left(\frac{\pi\xi}{2}\right) \frac{(2+\xi)l^{(\xi-1)}}{2^{\xi+4}\pi^2} \Gamma(\xi+2) \zeta_R(\xi+3) \frac{1}{L^{3+\xi}}. \quad (56)$$

Therefore the quantity $\Delta\nu^2$ defined in Eq. (54) can be written in the form,

$$\Delta\nu^2 = -\frac{A}{m_{\text{eff}}} \sin\left(\frac{\pi\xi}{2}\right) \frac{(3+\xi)(2+\xi)}{2^{\xi+6}\pi^4} \Gamma(\xi+2) \zeta_R(\xi+3) \left(\frac{l}{L}\right)^{\xi-1} \frac{1}{L^5}. \quad (57)$$

Considering the estimated result written in Eq. (55), together with the Eq. (51), we write the ratio $(l/L)^{\xi-1}$ in the following way

$$\left(\frac{l}{L}\right)^{\xi-1} = 0.34 \times 10^{-28} \frac{m_{\text{eff}}}{A} \frac{2^{\xi+6}\pi^4}{(3+\xi)(2+\xi) \sin\left(\frac{\pi\xi}{2}\right) \Gamma(\xi+2) \zeta_R(\xi+3)}, \quad (58)$$

where we have considered the error bar of C_{Cas} . Hence, from the experimental value of A/m_{eff} written in Eq. (55), the expression in Eq. (58) allows us to construct Table I. Note that we are taking the absolute value of the ratio l/L , since it is a positive quantity. As we can see from Table I, the bigger the value of ξ the smaller the ratio l/L . The biggest value is for $\xi = 3$, which is about $l/L \simeq 3.6 \times 10^{-14}$.

We emphasize that the analysis in Ref. [3] makes no assumptions about the nature of the quantum field. The data are simply better fitted by the electromagnetic quantum modes responsible for the Casimir effect. However, the error bar in C_{Cas} below Eq. (51) allows for the inclusion of other contributions, which could improve constraints on the Casimir force, including potential effects from additional quantum field modes.

Furthermore, we point out that the experimental analysis in Ref. [3] was not designed to test Lorentz symmetry violations, being instead based on the standard L^{-5} dependence for parallel plates. However, as previously noted, the experimental uncertainty in C_{Cas} may accommodate potential Lorentz-violating effects. We may therefore obtain a conservative estimate for l/L by assuming such effects lie within the experimental error margin. A dedicated experimental study would be required to establish more stringent constraints.

V. CONCLUDING REMARKS

The main objective of this paper was to analyze the vacuum energy and the generation of topological mass for a system composed by a massive self-interaction scalar quantum field in the scenario of a Hořava-Lifshitz-like model, and in this way to extend previous analysis developed in [37]. In this context, the vacuum energy was calculated considering that the field obeys Dirichlet boundary condition on two large parallel plates separated by a distance L . The energy spectrum is derived and using the ζ -function regularization approach we have calculated the renormalized effective potential, $V_{\text{eff}}^{\text{R}}(\Phi)$, given in (27) for an arbitrary value of the critical exponent ξ . The vacuum energy density is obtained from this potential in the vacuum state. Our result is presented in (28). We have explicitly shown that for even values of this parameter, this one-loop correction vanishes. Unfortunately, an analytical expression is not possible for general values of ξ . Moreover, the two-loop correction to the vacuum energy was presented in (40) for arbitrary value ξ , in the massive field case. Its massless limit, on the other hand, has been obtained in Eq. (41) and only gives a finite result for $\xi = 1$, the standard case where the Lorentz symmetry is preserved. However, for $\xi > 1$ the integral does not converge as a consequence of infrared divergences introduced by the model.

Another relevant calculation was developed in IV C, that is, the generation of topological mass. This observable is given by the second derivative with respect to the field Φ of the renormalized effective potential, prepared in the vacuum state. The corresponding expression was given in (45) as an integral representation for arbitrary value of ξ . We explicitly show that it goes to zero in the limit $mL \rightarrow \infty$ and vanishes for even value of the critical exponent.

In Fig.1 we have exhibited the graphs of the dimensionless vacuum energy density $E(mL) = 4\pi^2 L^4 \mathcal{E}_0$, as a function of mL , considering the values $\xi = 1, 3, 5, 7$. Additionally, the vacuum energy density for the case of a massless field is presented in Eq. (37), which shows the dependency on L and ξ , and reproduces the obtained results in Ref. [36].

In Fig.2 we have exhibited graphs for the dimensionless two-loop contribution to the vacuum energy density $\Delta E(mL) = \frac{128}{\lambda\pi^2} L^4 \mathcal{E}_0^\lambda$ as a function of mL , considering the values $\xi = 1, 3, 5, 7$. The graphs show that the correction goes to zero as $mL \rightarrow \infty$ (as it should be) and diverges as $mL \rightarrow 0$ (for $\xi > 1$), indicating the infrared divergences.

In the case of a massive field, its mass acquires a correction which depends on the critical exponent, ξ , on the parameter L and also on the self-interaction coupling constant λ . This correction is presented in Eq. (45). However, for $\xi > 1$, this expression for the topological mass diverges as $mL \rightarrow 0$, also indicating the presence of infrared divergences. This can be better seen in Eq. (49), which clearly converges only for $\xi = 1$. In contrast, for $mL \rightarrow \infty$ the topological mass goes to zero, as expected. This is shown in the graphs of Fig.3. The graph on the right shows that for $\xi = 5, 9$ the topological mass is negative and a vacuum stability analysis must take place in a model with interacting fields.

We have also provided an estimative for the ratio l/L by comparison with experimental results presented in Ref. [3]. The values of the ratio l/L are presented in Table I. It shows that the ratio l/L decreases as ξ increases, with the biggest value being about $l/L \simeq 3.6 \times 10^{-14}$. As a future work, we plan to look further into the issue of infrared divergences that appear in the massless scalar field case, and also analyze a system where two scalar fields interact.

It is worth emphasizing that the scalar field model considered in this work serves purely as a toy model for probing general features of Lorentz-violating effects on confined quantum fields. While scalar theories offer a technically tractable setting, it is well known that the extension of Lorentz-violating structures to electromagnetic fields is highly nontrivial due to the stringent constraints imposed by gauge invariance (see Ref. [54]). The admissible Lorentz-breaking operators in gauge theories differ significantly from those in scalar models, both in structure and physical implications. Studies involving HL-like theories with gauge and spinor fields confirm that each sector requires a specific treatment to preserve renormalizability and/or gauge invariance, as discussed for instance in Refs. [55, 56]. Therefore, the results presented here should be viewed as qualitative indications rather than direct predictions for electromagnetic phenomena.

Finally, in contrast to previous studies that focused on free scalar fields, in this work we incorporate a self-interaction potential and compute loop corrections to the vacuum energy up to two-loop order. We also investigate the generation of topological mass and provide phenomenological estimates based on experimental data. These aspects constitute significant extensions to prior HL-like scalar models, and uncover new features such as infrared divergences for $\xi > 1$ and dependence of the Casimir-like pressure on the interaction strength. Although our model is scalar and serves as a simplified toy model, it offers valuable qualitative insights into how Lorentz-violating structures may influence quantum vacuum effects.

Acknowledgments

The author H.M. is partially supported by the Brazilian agency National Council for Scientific and Technological Development (CNPq) under Grant No. 308049/2023-3.

Appendix A: Abel-Plana formula

In this appendix we use the Abel-Plana formula [13, 36, 46, 47],

$$\sum_{n=1}^{\infty} f(n) = \int_0^{\infty} dx f(x) - \frac{1}{2}f(0) + i \int_0^{\infty} dx \frac{f(ix) - f(-ix)}{e^{2\pi x} - 1}, \quad (\text{A.1})$$

to perform the sum in n present in Eq. (22). Hence, the generalized zeta function in Eq. (22) can be written as a sum of three contributions, namely,

$$\zeta(s) = \zeta_{\text{M}}(s) + \zeta_{\text{IP}}(s) + \zeta_0(s). \quad (\text{A.2})$$

The first contribution, $\zeta_{\text{M}}(s)$, reads,

$$\begin{aligned} \zeta_{\text{M}}(s) &= \frac{\Omega_3 \pi^{\frac{1}{2} + \xi - 2\xi s}}{8\xi b^{s - \frac{1}{2}} L^{2 + \xi - 2\xi s}} \frac{\Gamma\left(s - \frac{1}{2} - \frac{1}{\xi}\right) \Gamma\left(s - \frac{1}{2}\right)}{\Gamma(s) \Gamma\left(s + \frac{1}{2} - \frac{1}{\xi}\right)} \\ &\times \int_0^{\infty} dx (x^{2\xi} + U)^{\frac{1}{2} + \frac{1}{\xi} - s} {}_2F_1\left(1 - \frac{1}{\xi}, s - \frac{1}{2} - \frac{1}{\xi}, s + \frac{1}{2} - \frac{1}{\xi}, \frac{U}{x^{2\xi} + U}\right), \end{aligned} \quad (\text{A.3})$$

which is in fact the Minkowski contribution that comes from the integral in the first term on r.h.s. of Eq. (A.1). The second contribution comes from the second term on r.h.s. of Eq. (A.1) and is associated with the one plate case. This contribution is given by

$$\begin{aligned} \zeta_{\text{IP}}(s) &= -\frac{\Omega_3 \pi^{\frac{1}{2} + \xi - 2\xi s} U^{\frac{1}{2} + \frac{1}{\xi} - s}}{16\xi b^{s - \frac{1}{2}} L^{2 + \xi - 2\xi s}} \frac{\Gamma\left(s - \frac{1}{2}\right)}{\Gamma(s)} \\ &\times \frac{\Gamma\left(s - \frac{1}{2} - \frac{1}{\xi}\right)}{\Gamma\left(s + \frac{1}{2} - \frac{1}{\xi}\right)} {}_2F_1\left(1 - \frac{1}{\xi}, s - \frac{1}{2} - \frac{1}{\xi}, s + \frac{1}{2} - \frac{1}{\xi}, 1\right). \end{aligned} \quad (\text{A.4})$$

For the third contribution we have to separate the integral in the variable x into two intervals: from $[0, U^{\frac{1}{2\xi}}]$ and from $[U^{\frac{1}{2\xi}}, \infty)$. For the first interval and considering ξ an integer number, there is no contribution. In the second interval and considering ξ an integer number, the situation is more delicate. In this case we have $U^{\frac{1}{2\xi}} < x$, which yields,

$$\begin{aligned} f(ix) - f(-ix) &= 2i \sin\left(\frac{\pi\xi}{2} + \pi - \pi\xi s\right) \left[x^{2\xi} + (-1)^\xi U\right]^{\frac{1}{2} + \frac{1}{\xi} - s} \\ &\times {}_2F_1\left(1 - \frac{1}{\xi}, s - \frac{1}{2} - \frac{1}{\xi}, s + \frac{1}{2} - \frac{1}{\xi}, \frac{U}{U + (-1)^\xi (x)^{2\xi}}\right). \end{aligned} \quad (\text{A.5})$$

From the above expression we can infer that for ξ even, the difference above goes to zero, since we will eventually have to take $s \rightarrow 0$. Additionally, since the third term in the Abel-Plana formula is the one which originates the vacuum energy density, we see that for ξ even we have a vanishing vacuum energy density. Hence, we will investigate only the cases in which ξ is an odd number. Thus, for the third contribution in Eq. (A.2) that comes from the integral in the third term on the r.h.s. of Eq. (A.1), we have

$$\begin{aligned} \zeta_0(s) &= -\frac{\Omega_3 \sin\left[\pi\left(\frac{\xi}{2} + 1 - \xi s\right)\right]}{4\xi \pi^{2\xi s - \frac{1}{2} - \xi} b^{s - \frac{1}{2}} L^{2 + \xi - 2\xi s}} \frac{\Gamma\left(s - \frac{1}{2} - \frac{1}{\xi}\right) \Gamma\left(s - \frac{1}{2}\right)}{\Gamma(s) \Gamma\left(s + \frac{1}{2} - \frac{1}{\xi}\right)} \\ &\times \int_{U^{\frac{1}{2\xi}}}^{\infty} dx \frac{(x^{2\xi} - U)^{\frac{1}{2} + \frac{1}{\xi} - s}}{e^{2\pi x} - 1} {}_2F_1\left(1 - \frac{1}{\xi}, s - \frac{1}{2} - \frac{1}{\xi}, s + \frac{1}{2} - \frac{1}{\xi}, \frac{U}{U - x^{2\xi}}\right). \end{aligned} \quad (\text{A.6})$$

Thus, we have the generalized zeta function, Eq. (A.2), as a sum of three terms, namely, Eq. (A.3), (A.4) and (A.6).

The next step is to evaluate the generalized zeta function and its derivatives at $s = 0$, for each of the three terms separately. All the three terms are zero at $s = 0$, and by series expansion about $s = 0$ we obtain the derivatives as

$$\begin{aligned}\zeta'_M(0) &= \frac{\Omega_3 \pi^{\xi+1} b^{\frac{1}{2}} U^{\frac{1}{2} + \frac{3}{2\xi}}}{4(\xi+2)L^{\xi+2}} \int_0^\infty dy (y^{2\xi} + 1)^{\frac{1}{2} + \frac{1}{\xi}} F\left(1 - \frac{1}{\xi}, -\frac{1}{2} - \frac{1}{\xi}, \frac{1}{2} - \frac{1}{\xi}, \frac{1}{1+y^{2\xi}}\right), \\ \zeta'_{1P}(0) &= -\frac{\Omega_3 \pi^{\xi + \frac{1}{2}} b^{\frac{1}{2}} U^{\frac{1}{2} + \frac{1}{\xi}}}{16\xi b^{\frac{1}{\xi}} L^{\xi+2}} \Gamma\left(-\frac{1}{2} - \frac{1}{\xi}\right) \Gamma\left(\frac{1}{\xi}\right), \\ \zeta'_0(0) &= \sin\left(\frac{\pi\xi}{2}\right) \frac{\Omega_3 \pi^{1+\xi} b^{\frac{1}{2}}}{(\xi+2)L^{2+\xi}} \sum_{n=1}^{\infty} \int_{U^{\frac{1}{2\xi}}}^{\infty} dx \mathcal{F}(n, \xi, U, x).\end{aligned}\tag{A.7}$$

Note that in the first line of the above equation, we change the integration variable as $y^{2\xi} = x^{2\xi}/U$. Besides, this term is divergent and represents the contribution with no boundaries (no parallel plates, that is, the Minkowski contribution) and it should be discarded [36]. The contribution from the second line of the above equation is the contribution coming from one plate, which grows with positive powers of the mass present in U (see Eq. (29)) and, thus should be discarded. Finally, the third line gives the contribution which truly generates the vacuum energy density.

-
- [1] H. B. Casimir, *On the attraction of two perfectly conducting plates*, in *Proc. Kon. Ned. Akad. Wet.*, vol. 51, p. 793, 1948.
 - [2] M. J. Sparnaay, *Measurements of attractive forces between flat plates*, *Physica* **24** (1958) 751–764.
 - [3] G. Bressi, G. Carugno, R. Onofrio, and G. Ruoso, *Measurement of the casimir force between parallel metallic surfaces*, *Phys. Rev. Lett.* **88** (Jan, 2002) 041804.
 - [4] W. J. Kim, M. Brown-Hayes, D. A. R. Dalvit, J. H. Brownell, and R. Onofrio, *Anomalies in electrostatic calibrations for the measurement of the casimir force in a sphere-plane geometry*, *Phys. Rev. A* **78** (Aug, 2008) 020101.
 - [5] S. K. Lamoreaux, *Demonstration of the casimir force in the 0.6 to 6 μ m range*, *Phys. Rev. Lett.* **78** (Jan, 1997) 5–8.
 - [6] S. Lamoreaux, *Erratum: Demonstration of the casimir force in the 0.6 to 6 μ m range [phys. rev. lett. 78, 5 (1997)]*, *Physical Review Letters* **81** (1998), no. 24 5475.
 - [7] U. Mohideen and A. Roy, *Precision measurement of the Casimir force from 0.1 to 0.9 micrometers*, *Phys. Rev. Lett.* **81** (1998) 4549–4552, [[physics/9805038](#)].
 - [8] V. M. Mostepanenko, *New experimental results on the casimir effect*, *Brazilian Journal of Physics* **30** (2000), no. 2 309–315.
 - [9] Q. Wei, D. A. R. Dalvit, F. C. Lombardo, F. D. Mazzitelli, and R. Onofrio, *Results from electrostatic calibrations for measuring the casimir force in the cylinder-plane geometry*, *Phys. Rev. A* **81** (May, 2010) 052115.
 - [10] A. Romeo and A. A. Saharian, *Casimir effect for scalar fields under Robin boundary conditions on plates*, *J. Phys. A* **35** (2002) 1297–1320, [[hep-th/0007242](#)].
 - [11] G. Aleixo and H. F. S. Mota, *Thermal Casimir effect for the scalar field in flat spacetime under a helix boundary condition*, *Phys. Rev. D* **104** (2021), no. 4 045012, [[arXiv:2105.0822](#)].
 - [12] C. A. Escobar, A. Martín-Ruiz, R. Linares, and J. M. Silva, *A coherent state approach to the Casimir effect for a massive scalar field in a noncommutative spacetime*, *Annals Phys.* **460** (2024) 169570.
 - [13] M. Bordag, G. L. Klimchitskaya, U. Mohideen, and V. M. Mostepanenko, *Advances in the Casimir effect*, vol. 145. OUP Oxford, 2009.
 - [14] K. A. Milton, *The Casimir effect: physical manifestations of zero-point energy*. World Scientific, 2001.
 - [15] V. Mostepanenko, N. Trunov, and R. Znajek, *The Casimir Effect and Its Applications*. Oxford science publications. Clarendon Press, 1997.
 - [16] V. A. Kostelecký and S. Samuel, *Spontaneous breaking of lorentz symmetry in string theory*, *Physical Review D* **39** (1989), no. 2 683.
 - [17] D. Colladay and V. A. Kostelecký, *CPT violation and the standard model*, *Phys. Rev. D* **55** (Jun, 1997) 6760–6774.
 - [18] A. J. D. Farias Junior and H. F. Mota Santana, *Loop correction to the scalar Casimir energy density and generation of topological mass due to a helix boundary condition in a scenario with Lorentz violation*, *Int. J. Mod. Phys. D* **31** (2022), no. 16 2250126, [[arXiv:2204.0940](#)].
 - [19] M. Cruz, E. Bezerra de Mello, and A. Petrov, *Thermal corrections to the casimir energy in a lorentz-breaking scalar field theory*, *Modern Physics Letters A* **33** (05, 2018) 37.
 - [20] A. F. Santos and F. C. Khanna, *Corrections Due to Lorentz Violation, Finite Temperature, and Magnetic Field for the Casimir Effect of a Massive Scalar Field*, *Int. J. Theor. Phys.* **61** (2022), no. 4 96.
 - [21] R. A. Dantas, H. F. S. Mota, and E. R. Bezerra de Mello, *Bosonic casimir effect in an aether-like lorentz-violating scenario with higher order derivatives*, *Universe* **9** (2023), no. 5 241.
 - [22] D. Colladay and V. A. Kostelecký, *Lorentz-violating extension of the standard model*, *Phys. Rev. D* **58** (Oct, 1998) 116002.
 - [23] A. Anisimov, T. Banks, M. Dine, and M. Graesser, *Comments on noncommutative phenomenology*, *Phys. Rev. D* **65** (2002) 085032, [[hep-ph/0106356](#)].

- [24] C. E. Carlson, C. D. Carone, and R. F. Lebed, *Bounding noncommutative qcd*, *Physics Letters B* **518** (2001), no. 1-2 201–206.
- [25] J. L. Hewett, F. J. Petriello, and T. G. Rizzo, *Signals for noncommutative interactions at linear colliders*, *Physical Review D* **64** (2001), no. 7 075012.
- [26] O. Bertolami and L. Guisado, *Noncommutative field theory and violation of translation invariance*, *Journal of High Energy Physics* **2003** (2003), no. 12 013.
- [27] V. A. Kostelecký, R. Lehnert, and M. J. Perry, *Spacetime-varying couplings and lorentz violation*, *Physical Review D* **68** (2003), no. 12 123511.
- [28] L. Anchordoqui and H. Goldberg, *Time variation of the fine structure constant driven by quintessence*, *Physical Review D* **68** (2003), no. 8 083513.
- [29] O. Bertolami, *Lorentz invariance and the cosmological constant*, *Classical and Quantum Gravity* **14** (1997), no. 10 2785.
- [30] J. Alfaro, H. A. Morales-Tecotl, and L. F. Urrutia, *Quantum gravity corrections to neutrino propagation*, *Physical Review Letters* **84** (2000), no. 11 2318.
- [31] J. Alfaro, H. A. Morales-Tecotl, and L. F. Urrutia, *Loop quantum gravity and light propagation*, *Physical Review D* **65** (2002), no. 10 103509.
- [32] P. Hořava, *Quantum gravity at a lifshitz point*, *Physical Review D* **79** (2009), no. 8 084008.
- [33] D. Anselmi, *Weighted power counting and lorentz violating gauge theories. i: General properties*, *Annals of Physics* **324** (2009), no. 4 874–896.
- [34] D. Anselmi, *Weighted power counting and lorentz violating gauge theories. ii: Classification*, *Annals of Physics* **324** (2009), no. 5 1058–1077.
- [35] A. F. Ferrari, H. O. Girotti, M. Gomes, A. Y. Petrov, and A. J. da Silva, *Horava-Lifshitz modifications of the Casimir effect*, *Mod. Phys. Lett. A* **28** (2013) 1350052, [[arXiv:1006.1635](#)].
- [36] I. M. Ulion, E. B. de Mello, and A. Yu. Petrov, *Casimir effect in horava-lifshitz-like theories*, *International Journal of Modern Physics A* **30** (2015), no. 36 1550220.
- [37] R. V. Maluf, D. M. Dantas, and C. A. S. Almeida, *The Casimir effect for the scalar and Elko fields in a Lifshitz-like field theory*, *Eur. Phys. J. C* **80** (2020), no. 5 442, [[arXiv:1905.0482](#)].
- [38] R. Jackiw, *Functional evaluation of the effective potential*, *Phys. Rev. D* **9** (1974) 1686.
- [39] L. H. Ryder, *Quantum field theory*. Cambridge university press, 1996.
- [40] D. J. Toms, *Symmetry Breaking and Mass Generation by Space-time Topology*, *Phys. Rev. D* **21** (1980) 2805.
- [41] M. B. Cruz, E. R. Bezerra de Mello, and H. F. Santana Mota, *Casimir energy and topological mass for a massive scalar field with Lorentz violation*, *Phys. Rev. D* **102** (2020), no. 4 045006, [[arXiv:2005.0951](#)].
- [42] P. J. Porfírio, H. F. Santana Mota, and G. Q. Garcia, *Ground state energy and topological mass in spacetimes with nontrivial topology*, *Int. J. Mod. Phys. D* **30** (2021), no. 08 2150056, [[arXiv:1908.0051](#)].
- [43] A. J. D. F. Junior and H. F. S. Mota, *Casimir effect, loop corrections, and topological mass generation for interacting real and complex scalar fields in minkowski spacetime with different conditions*, *Phys. Rev. D* **107** (Jun, 2023) 125019.
- [44] S. W. Hawking, *Zeta Function Regularization of Path Integrals in Curved Space-Time*, *Commun. Math. Phys.* **55** (1977) 133.
- [45] I. S. Gradshteyn and I. M. Ryzhik, *Table of integrals, series, and products*. Academic press, 2014.
- [46] L. H. Ford, *Vacuum polarization in a nonsimply connected spacetime*, *Phys. Rev. D* **21** (Feb, 1980) 933–948.
- [47] A. A. Saharian, *The generalized abel-plana formula with applications to bessel functions and casimir effect*, 2007.
- [48] M. Abramowitz and I. A. Stegun, *Handbook of mathematical functions dover publications*, New York **361** (1965).
- [49] M. B. Cruz, E. R. B. de Mello, and A. Y. Petrov, *Casimir effects in lorentz-violating scalar field theory*, *Phys. Rev. D* **96** (Aug, 2017) 045019.
- [50] M. Bordag, U. Mohideen, and V. M. Mostepanenko, *New developments in the casimir effect*, *Physics reports* **353** (2001), no. 1-3 1–205.
- [51] G. B. Arfken, H. J. Weber, and F. E. Harris, *Mathematical methods for physicists: a comprehensive guide*. Academic press, 2011.
- [52] D. J. Toms, *Interacting Twisted and Untwisted Scalar Fields in a Nonsimply Connected Space-time*, *Annals Phys.* **129** (1980) 334.
- [53] F. Pascoal, L. Oliveira, F. Rosa, and C. Farina, *Estimate for the size of the compactification radius of a one extra dimension universe*, *Brazilian Journal of Physics* **38** (2008) 581–586.
- [54] V. A. Kostelecký and M. Mewes, *Electrodynamics with lorentz-violating operators of arbitrary dimension*, *Phys. Rev. D* **80** (2009) 015020, [[arXiv:0905.0031](#)].
- [55] C. F. Farias, M. Gomes, J. R. Nascimento, A. Y. Petrov, and A. J. da Silva, *Effective potential for horava-lifshitz-like theories*, *Phys. Rev. D* **85** (2012) 127701, [[arXiv:1112.2081](#)].
- [56] C. F. Farias, J. R. Nascimento, and A. Y. Petrov, *On the effective potential for horava-lifshitz-like theories with the arbitrary critical exponent*, *Phys. Lett. B* **719** (2013) 196–199, [[arXiv:1211.1222](#)].